An Analysis of the Error Characteristics of Two Time of Arrival Localization Techniques

T. Sathyan
ICT Center
CSIRO
Marsfield, NSW, Australia
saji.sathyan@csiro.au

M. Hedley
ICT Center
CSIRO
Marsfield, NSW, Australia
mark.hedley@csiro.au

M. Mallick
Georgia Tech Research Institute
Georgia Institute of Technology
Atlanta, GA 30332, USA
mahendra.mallick@gtri.gatech.edu

Abstract – *Accurate local positioning systems usually use a network of anchor nodes at known locations to track mobile nodes based on the measurement of the time of arrival (TOA) at anchor nodes of beacon signals transmitted by the mobile nodes. To localize the mobile node either TOA processing, where the unknown transmit time is estimated along with the node location, or time difference of arrival (TDOA) processing, where the transmit time is eliminated before estimating the node location, can be used. We show that the position error bound of both these formulations are the same by analyzing the Cramér-Rao lower bound. When processing data collected in field trials, however, we observed that the TOA processing yields better localization accuracy, and explain this behavior using differential geometry-based curvature measures that show that the TDOA cost function has greater degree of non-linearity.*

Keywords: Wireless sensor networks, localization, TOA-ranging, pseudo-range, Cramér-Rao lower bound, differential geometry, curvature measures of nonlinearity, TDOA.

1 Introduction

GPS is one of the most widely used localization systems due to its wide availability and low cost. For many applications, however, GPS is not suitable for a variety of reasons including being unavailable (e.g., indoors), having too low accuracy (particularly in multipath environments) or too low update rate. For this reason there has been much recent work in developing local positioning systems that overcome these limitations.

Many localization systems, including GPS, are based on the measurement of the time of arrival (TOA) of a transmitted signal as it can provide better multipath resilience compared to competing techniques such as received signal strength or angle of arrival localization systems [11]. Local positioning systems consist of anchor nodes, whose locations are known, and mobile nodes, whose locations are estimated using the networks of anchor nodes. In network-centric systems, localization is performed by measuring the TOA of a beacon emitted by the mobile node at the anchors. In mobile-centric systems (e.g., GPS) the mobile node measures the TOA of the beacons from the anchors and localizes itself.

If both the mobile node and anchors in the system are time and frequency synchronized, including a correction for the propagation delay through the system electronics, then based on the measured TOA the time of flight (TOF), hence the ranges, between the mobile node and each anchor is readily obtained. If, however, all the anchors in the system are synchronized and only the anchor nodes (as in GPS) or the mobile nodes transmit a beacon, then the measured TOA corresponds to a pseudo-TOF (or pseudo-range, when multiplied by the speed of light), which is the actual TOF plus an unknown offset (usually the transmit time) that is common to all anchors.[1] Most local positioning systems only perform TOA measurement in the anchor nodes so that the mobile nodes (tags) are smaller, lower power and lower cost.

Calculating the location of the mobile node using measured pseudo-ranges can be formulated in two ways depending on how the unknown range-offset is treated. In one formulation, called TOA processing, the unknown offset is estimated along with the mobile node location. This is used in GPS [7] and allows the receiver to synchronize its clock to the global time. In the other approach, the unknown offset is treated as a nuisance parameter and eliminated by considering the time difference of arrival (TDOA). This is called TDOA processing.

The pseudo-range measurement equations that relate the locations of the anchors and the mobile node are nonlinear. One technique to estimate the mobile location is to linearize the measurement equations and use linear least squares algorithm to solve the linearized equations. It was shown in [13] that the position estimate and its error covariance resulting from TOA and TDOA processing are identical if the linearized TOA equations are considered. It is clear, however, that directly localizing the mobile node using the nonlinear measurement equations will result in better accuracy

[1] TOF or pseudo-TOF can be easily converted to the range or pseudo-range. Hence we use TOF and range, and pseudo-TOF and pseudo-range, interchangeably.

compared to the linearized processing.

In this paper we show that the position error bounds of the nonlinear TOA and TDOA processing are the same by analyzing the Cramér-Rao lower bound (CRLB) of the two formulations. Thus one would expect to obtain the same localization accuracy, irrespective of the type of processing selected. When we tested these two processing methods on data collected in field trials, using a local positioning system that we have developed, we found that the TOA processing resulted in significantly better localization accuracy compared to the TDOA processing. We explain this observation by quantifying the nonlinearity of the measurement functions and by showing that the nonlinearity of the TDOA processing is higher compared to TOA processing.

In the next section we introduce the two pseudo-range localization formulations that are considered in this paper. In Section 3 we show that the CRLB of the position estimation of the two approaches are the same. Differential geometry curvature measures for nonlinearity are explained briefly in Section 4. Field trial results comparing the performance the two approaches, along with an analysis of the curvature measures for this trial, are presented in Section 5.

2 Localization using pseudo-ranges

Assume that in a particular scenario there are N anchor nodes whose known locations are given by $\mathbf{p}_i = [x_i, y_i]^T, i = 1, 2, \ldots, N$. Further assume that these anchors are perfectly time and frequency synchronized. These anchors measure the TOA of a wideband pulse emitted by the mobile node. We can write the TOA t_i at the ith anchor as

$$t_i = t_0 + \frac{\|\mathbf{p} - \mathbf{p}_i\|}{c} + n_i \qquad i = 1, 2, 3, \ldots, N \tag{1}$$

where t_0 is the unknown transmit time, $\mathbf{p} = [x, y]^T$ is the unknown location of the mobile node, c is the speed of light, and n_i is the TOA measurement noise, which is assumed to be zero-mean Gaussian distributed with standard deviation σ_i.

The TOA measurements can be easily converted to the range domain, with the pseudo-range measurement r_i of anchor i given by

$$r_i = r_0 + \|\mathbf{p} - \mathbf{p}_i\| + v_i \qquad i = 1, 2, 3, \ldots, N \tag{2}$$

where $r_0 = ct_0$ is the unknown range offset.

Given N pseudo-range measurements r_i, the objective of the localization problem is to find the unknown location of the mobile node $\mathbf{p}$. For many applications the range offset r_0 is of little practical use and hence, it is often not required to be estimated. In GPS, however, the range offset (or the corresponding time offset) allows the global time to be tracked at the receiver. Depending on how the range offset parameter is treated, two formulations for the localization of mobile node are possible.

2.1 Approach I - TDOA Processing

In the first approach the range offset is considered as a nuisance parameter and is eliminated from the estimation problem. This can be done by considering the TDOA, or equivalently the pseudo-range difference, equations. Without loss of generality assume anchor 1 as the reference anchor and then we can form $N - 1$ range difference measurements $r_{i1} = r_i - r_1, i = 2, 3, \cdots, N$. That is

$$r_{i1} = \|\mathbf{p} - \mathbf{p}_i\| - \|\mathbf{p} - \mathbf{p}_1\| + v_{i1} \quad i = 2, 3, \cdots, N \tag{3}$$

where $v_{i1} = v_i - v_1$.

The vector of range difference measurements $\mathbf{r}_d = [r_{21}, r_{31}, \ldots, r_{N1}]^T$ has a joint conditional Gaussian distribution. That is

$$p(\mathbf{r}_d|\mathbf{q}) = \mathcal{N}(\mathbf{r}_d; \boldsymbol{\mu}_{TD}, R_{TD}) \tag{4}$$

where

$$\boldsymbol{\mu}_{TD} = \begin{bmatrix} \|\mathbf{p} - \mathbf{p}_2\| - \|\mathbf{p} - \mathbf{p}_1\| \\ \|\mathbf{p} - \mathbf{p}_3\| - \|\mathbf{p} - \mathbf{p}_1\| \\ \vdots \\ \|\mathbf{p} - \mathbf{p}_N\| - \|\mathbf{p} - \mathbf{p}_1\| \end{bmatrix} \tag{5}$$

and

$$R_{TD} = \begin{bmatrix} \sigma_1^2 + \sigma_2^2 & \sigma_1^2 & \ldots & \sigma_1^2 \\ \sigma_1^2 & \sigma_1^2 + \sigma_3^2 & \ldots & \sigma_1^2 \\ \vdots & \vdots & \vdots & \vdots \\ \sigma_1^2 & \sigma_1^2 & \ldots & \sigma_1^2 + \sigma_N^2 \end{bmatrix} \tag{6}$$

The maximum likelihood (ML) location estimate is then given by

$$\mathbf{p}_{ML} = \arg\max_{\mathbf{p}} \log\, p(\mathbf{r}_d|\mathbf{p}) \tag{7}$$

2.2 Approach II - TOA Processing

In the second approach the range offset is estimated along with the position of the mobile node. Let the unknown parameters be grouped into $\mathbf{q} = [\mathbf{p}, r_0]^T$. Since the pseudo-range measurements in different anchors are independent, the vector of pseudo-range measurements $\mathbf{r} = [r_1, r_2, \ldots, r_N]^T$ has the following conditional distribution.

$$p(\mathbf{r}|\mathbf{q}) = \mathcal{N}(\mathbf{r}; \boldsymbol{\mu}_T, R_T) \tag{8}$$

where

$$\boldsymbol{\mu}_T = \begin{bmatrix} r_0 + \|\mathbf{p} - \mathbf{p}_1\| \\ r_0 + \|\mathbf{p} - \mathbf{p}_2\| \\ \vdots \\ r_0 + \|\mathbf{p} - \mathbf{p}_N\| \end{bmatrix} \quad R_T = \begin{bmatrix} \sigma_1^2 & 0 & \ldots & 0 \\ 0 & \sigma_2^2 & \ldots & 0 \\ \vdots & \vdots & \vdots & \vdots \\ 0 & 0 & \ldots & \sigma_N^2 \end{bmatrix} \tag{9}$$

As in the previous case the ML estimate of the unknown parameter vector $\mathbf{q}$ is given by

$$\mathbf{q}_{ML} = \arg\max_{\mathbf{p}} \log\, p(\mathbf{r}|\mathbf{q}) \tag{10}$$

and the mobile node location can be easily extracted from $\mathbf{q}$.

2.3 Solution techniques

The ML estimation formulations in (7) and (10) are nonlinear optimization problems and do not have closed-form solutions. A straightforward approach is to linearize the cost function using a Taylor series approximation and iteratively solve the resulting linear optimization problem [4].

A number of solutions [3][6][14] have been proposed for localization using range difference measurements, i.e., for Approach I. These algorithms derive the relationship between the range differences and the node locations using the geometry and introduce what is called an equation error to account for noisy range difference measurements. Then the equation error is minimized to find the mobile node location. These algorithms cannot be readily converted to solve Approach II, because of the unknown range-offset.

In our experiments we used the iterative least squares (ILS) algorithm [1] to solve the ML formulations in (7) and (10). Starting from an initial solution, the ILS algorithm updates the estimate using a first-order Taylor series approximation of the measurement equations until there is no more improvement in the accuracy of the location estimate or the desired accuracy is achieved. An initial solution for the ILS algorithm can be obtained by considering the linearized pseudo-range equations as follows.

Consider the following noise-free pseudo-range equation:

$$r_i = r_0 + \| \mathbf{p} - \mathbf{p}_i \| \tag{11}$$

$$= r_0 + \sqrt{(x - x_i)^2 + (y - y_i)^2} \tag{12}$$

After squaring the noise-free pseudo-range equations and rearranging the terms and then by subtracting the equation corresponding to that of anchor node 1 from that of all the other anchors, we will get the following $N-1$ equations:

$$2x_{i1} + 2y_{i1}y - 2r_{i1}r_0 = k_{i1} \qquad i = 2, 3, \cdots, N \tag{13}$$

where $x_{i1} = x_i - x_1$, $y_{i1} = y_i - y_1$, $r_{i1} = r_i - r_1$, and $k_{i1} = x_i^2 + y_i^2 - x_1^2 - y_1^2 - r_i^2 + r_1^2$. We can write the above $N-1$ equations in a matrix form as

$$P\mathbf{q} = \boldsymbol{\beta} \tag{14}$$

where $\mathbf{q} = [x, y, r_0]^T$,

$$P = \begin{bmatrix} 2x_{21} & 2y_{21} & -2r_{21} \\ 2x_{31} & 2y_{31} & -2r_{31} \\ \vdots & \vdots & \vdots \\ 2x_{N1} & 2x_{N1} & -2r_{N1} \end{bmatrix} \quad \boldsymbol{\beta} = \begin{bmatrix} k_{21} \\ k_{31} \\ \vdots \\ k_{N1} \end{bmatrix} \tag{15}$$

Therefore an initial solution for $\mathbf{q}$ is

$$\mathbf{q}^* = P^\dagger \boldsymbol{\beta} \tag{16}$$

where $P^\dagger$ refers to the pseudo-inverse of matrix P. Note that the ILS for Approach I can be initialized with the first two elements of $\mathbf{q}^*$.

3 Cramér-Rao Lower Bound

The CRLB provides a lower bound on the covariance that is achievable by any unbiased estimation algorithm [8] and often used to benchmark the estimation performance. Let $\mathbf{x} \in \mathbb{R}^n$ be the parameter of interest and $\hat{\mathbf{x}}$ an estimate of it obtained from measurements $\mathbf{z}$. Then the error covariance $\mathbb{E}\{(\mathbf{x} - \hat{\mathbf{x}})(\mathbf{x} - \hat{\mathbf{x}})^T\}$ is bounded by

$$\mathbb{E}\{(\mathbf{x} - \hat{\mathbf{x}})(\mathbf{x} - \hat{\mathbf{x}})^T\} \geq F^{-1} \tag{17}$$

where F is the Fisher information matrix (FIM) and the matrix inequality $A \geq B$ means that the matrix $A - B$ is positive semi-definite. The (i, j)th element of the FIM is defined as [8]

$$[F]_{ij} = -\mathbb{E}\left\{ \frac{\partial^2 \log p(\mathbf{z}|\mathbf{x})}{\partial x_i \partial x_j} \right\} \quad i, j = 1, 2, \cdots, n \tag{18}$$

We now derive the CRLB for the two pseudo-range localization formulations and show that the position components of both the bounds are the same, meaning that it is possible to achieve the same localization error performance using the two formulations.

3.1 FIM - TDOA Processing

In this case the unknown parameter vector $\mathbf{q}$ has two elements x and y, hence, the FIM is a 2×2 matrix. Let the FIM be

$$F_2 = -\begin{bmatrix} [F_2]_{11} & [F_2]_{12} \\ [F_2]_{21} & [F_2]_{22} \end{bmatrix} \tag{19}$$

where

$$[F_2]_{11} = \mathbb{E}\left\{ \frac{\partial^2 \log p(\mathbf{r}_d|\mathbf{p})}{\partial x^2} \right\} \tag{20}$$

$$[F_2]_{22} = \mathbb{E}\left\{ \frac{\partial^2 \log p(\mathbf{r}_d|\mathbf{p})}{\partial y^2} \right\} \tag{21}$$

$$[F_2]_{12} = [F_2]_{21} = \mathbb{E}\left\{ \frac{\partial^2 \log p(\mathbf{r}_d|\mathbf{p})}{\partial x \partial y} \right\} \tag{22}$$

Given the likelihood function (4), we can show that (see Appendix A)

$$[F_2]_{11} = \sum_{i=1}^{N} \frac{1}{\sigma_i^2} \frac{(x - x_i)^2}{\| \mathbf{p}_i - \mathbf{p} \|^2} - \frac{1}{\sigma} \sum_{i=1}^{N} \sum_{j=1}^{N} \frac{1}{\sigma_i^2 \sigma_j^2} \frac{(x - x_i)(x - x_j)}{\| \mathbf{p}_i - \mathbf{p} \| \| \mathbf{p}_j - \mathbf{p} \|} \tag{23}$$

$$[F_2]_{22} = \sum_{i=1}^{N} \frac{1}{\sigma_i^2} \frac{(y - y_i)^2}{\| \mathbf{p}_i - \mathbf{p} \|^2} - \frac{1}{\sigma} \sum_{i=1}^{N} \sum_{j=1}^{N} \frac{1}{\sigma_i^2 \sigma_j^2} \frac{(y - y_i)(y - y_j)}{\| \mathbf{p}_i - \mathbf{p} \| \| \mathbf{p}_j - \mathbf{p} \|} \tag{24}$$

$$[F_2]_{12} = [F_2]_{21} \tag{25}$$

$$= \sum_{i=1}^{N} \frac{1}{\sigma_i^2} \frac{(x-x_i)(y-y_i)}{\|\mathbf{p}_i - \mathbf{p}\|^2} - \frac{1}{\sigma} \sum_{i=1}^{N} \sum_{j=1}^{N} \frac{1}{\sigma_i^2 \sigma_j^2} \frac{(x-x_i)(y-y_j)}{\|\mathbf{p}_i - \mathbf{p}\| \|\mathbf{p}_j - \mathbf{p}\|} \tag{26}$$

where $\sigma = \sum_{i=1}^{N} \sigma_i$.

3.2 FIM - TOA Processing

The FIM in this case is a 3×3 matrix, since the parameter vector $\mathbf{q}$ has three elements x, y, and r_0. It is given by

$$F_3 = - \begin{bmatrix} [F_3]_{11} & [F_3]_{12} & [F_3]_{13} \\ [F_3]_{21} & [F_3]_{22} & [F_3]_{23} \\ [F_3]_{31} & [F_3]_{32} & [F_3]_{33} \end{bmatrix} \tag{27}$$

where

$$[F_3]_{11} = \mathbb{E}\left\{ \frac{\partial^2 \log p(\mathbf{r}|\mathbf{q})}{\partial x^2} \right\} \tag{28}$$

$$[F_3]_{22} = \mathbb{E}\left\{ \frac{\partial^2 \log p(\mathbf{r}|\mathbf{q})}{\partial y^2} \right\} \tag{29}$$

$$[F_3]_{12} = [F_3]_{21} = \mathbb{E}\left\{ \frac{\partial^2 \log p(\mathbf{r}|\mathbf{q})}{\partial x \partial y} \right\} \tag{30}$$

$$[F_3]_{13} = [F_3]_{31} = \mathbb{E}\left\{ \frac{\partial^2 \log p(\mathbf{r}|\mathbf{q})}{\partial x \partial r_0} \right\} \tag{31}$$

$$[F_3]_{23} = [F_3]_{32} = \mathbb{E}\left\{ \frac{\partial^2 \log p(\mathbf{r}|\mathbf{q})}{\partial y \partial r_0} \right\} \tag{32}$$

Assume that F_3 is partitioned as follows

$$F_3 = \begin{bmatrix} A & \mathbf{b} \\ \mathbf{b}^T & a \end{bmatrix} \tag{33}$$

where

$$A = \begin{bmatrix} [F_3]_{11} & [F_3]_{12} \\ [F_3]_{21} & [F_3]_{22} \end{bmatrix} \quad \mathbf{b} = \begin{bmatrix} [F_3]_{13} \\ [F_3]_{23} \end{bmatrix} \quad a = [F_3]_{33} \tag{34}$$

With the above partitioning the inverse of F_3, which is the CRLB, can be written as

$$F_3^{-1} = \begin{bmatrix} \tilde{A}^{-1} & -\frac{1}{k} A^{-1}\mathbf{b} \\ -\frac{1}{k}\mathbf{b}^T A^{-1} & \frac{1}{k} \end{bmatrix} \tag{35}$$

where $\tilde{A} = A - \frac{1}{a}\mathbf{b}\mathbf{b}^T$ and $k = a - \mathbf{b}^T A^{-1}\mathbf{b}$.

Elements of $\tilde{A}$ can be readily evaluated and can be shown to be equal to the elements of F_2. That is

$$\tilde{A} = F_2 \tag{36}$$

Since the position components of the CRLB in the second approach is given by $\tilde{A}^{-1}$ and that in the first approach by F_2, the equality of these matrices show that the position estimates obtained using the two approaches have the same lower bound.

4 Differential Geometry Measures for Nonlinearity

Simple relative curvature measures were developed in [2] to quantify the nonlinearity of a model function based on differential geometry. These measures were developed to quantify the adequacy of a linear approximation and its effects on the estimation of the parameter of interest. One of the measures, the parameter-effects curvature (PEC), quantifies the nonlinearity due to the particular parametrization of the model and the other, the intrinsic curvature (IC), quantifies the nonlinearity inherent to the model function.

Assume that $\mathbf{x}$ is a $N \times 1$ vector consisting of the unknown parameters. $\mathbf{f}(\mathbf{x})$ is vector function of length M. Then the second order Taylor series expansion of $\mathbf{f}(\mathbf{x})$ around $\hat{\mathbf{x}}$, an estimate of $\mathbf{x}$, is given by

$$\mathbf{f}(\mathbf{x}) = \mathbf{f}(\hat{\mathbf{x}}) + \dot{F}(\hat{\mathbf{x}})(\mathbf{x}-\hat{\mathbf{x}}) + \frac{1}{2}(\mathbf{x}-\hat{\mathbf{x}})^T \ddot{F}(\hat{\mathbf{x}})(\mathbf{x}-\hat{\mathbf{x}}) \tag{37}$$

where $\dot{F}(\hat{\mathbf{x}})$ is a matrix of size $M \times N$, whose (i,j)th element is given by

$$[\dot{F}(\hat{\mathbf{x}})]_{ij} = \left. \frac{\partial f_i(\mathbf{x})}{\partial x_j} \right|_{\mathbf{x}=\hat{\mathbf{x}}} \tag{38}$$

The quadratic term is a symbolic representation for an M-dimensional vector whose mth element is defined by $(\mathbf{x} - \hat{\mathbf{x}})^T \ddot{F}_m(\hat{\mathbf{x}})(\mathbf{x} - \hat{\mathbf{x}})$, where $\ddot{F}_m(\mathbf{x})$ is called the mth face of $\ddot{F}(\mathbf{x})$ [12] is an $N \times N$ matrix, whose (i,j)th element is given by

$$[\ddot{F}_m(\hat{\mathbf{x}})]_{ij} = \left. \frac{\partial^2 f_m(\mathbf{x})}{\partial x_i \partial x_j} \right|_{\mathbf{x}=\hat{\mathbf{x}}} \tag{39}$$

Define $M \times 1$ velocity vectors as [2]

$$\dot{F}_i(\hat{\mathbf{x}}) = \left[\left. \frac{\partial f_1(\mathbf{x})}{\partial x_i} \right|_{\mathbf{x}=\hat{\mathbf{x}}}, \left. \frac{\partial f_2(\mathbf{x})}{\partial x_i} \right|_{\mathbf{x}=\hat{\mathbf{x}}}, \cdots, \left. \frac{\partial f_M(\mathbf{x})}{\partial x_i} \right|_{\mathbf{x}=\hat{\mathbf{x}}} \right]^T \tag{40}$$

with

$$\dot{F}(\hat{\mathbf{x}}) = \left[\dot{F}_1(\mathbf{x}), \dot{F}_2(\mathbf{x}), \cdots, \dot{F}_M(\mathbf{x}) \right]^T \tag{41}$$

Also define $M \times 1$ symmetric acceleration vectors as

$$\ddot{F}_{ij}(\hat{\mathbf{x}}) = \left[\left. \frac{\partial^2 f_1(\mathbf{x})}{\partial x_i \partial x_j} \right|_{\mathbf{x}=\hat{\mathbf{x}}}, \left. \frac{\partial f_2(\mathbf{x})}{\partial x_i \partial x_j} \right|_{\mathbf{x}=\hat{\mathbf{x}}}, \cdots, \left. \frac{\partial^2 f_M(\mathbf{x})}{\partial x_i \partial x_j} \right|_{\mathbf{x}=\hat{\mathbf{x}}} \right]^T \tag{42}$$

where $i, j = 1, 2, \ldots, M$.

The projection matrix is defined as

$$P = \dot{F}(\mathbf{x})(\dot{F}(\mathbf{x})'\dot{F}(\mathbf{x}))^{-1}\dot{F}(\mathbf{x})' \tag{43}$$

Using the projection matrix we can decompose the acceleration vectors into the tangential and normal planes. Let $\ddot{f}_{ij}^{\mathrm{T}}(\tilde{\mathbf{x}})$ be the tangential component and $\ddot{f}_{ij}^{\mathrm{N}}(\tilde{\mathbf{x}})$ be the normal component of the acceleration vector.

$$\ddot{f}_{ij}^{\mathrm{T}}(\tilde{\mathbf{x}}) = P\ddot{f}_{ij}(\tilde{\mathbf{x}}) \qquad i, j = 1, 2, \ldots, N \tag{44}$$

$$\ddot{f}_{ij}^{\mathrm{N}}(\tilde{\mathbf{x}}) = (I - P)\ddot{f}_{ij}(\tilde{\mathbf{x}}) \qquad i, j = 1, 2, \ldots, N \tag{45}$$

The relative PEC K_δ^{T} and the IC K_δ^{N}, in the direction of $\boldsymbol{\delta}$ are defined as [2]

$$K_\delta^{\mathrm{T}} = \frac{\| \boldsymbol{\delta}^T \ddot{F}^{\mathrm{T}}(\hat{\mathbf{x}})\boldsymbol{\delta} \|}{\| \dot{F}^{\mathrm{T}}(\hat{\mathbf{x}})\boldsymbol{\delta} \|^2} \tag{46}$$

$$K_\delta^{\mathrm{N}} = \frac{\| \boldsymbol{\delta}^T \ddot{F}^{\mathrm{N}}(\hat{\mathbf{x}})\boldsymbol{\delta} \|}{\| \dot{F}^{\mathrm{T}}(\hat{\mathbf{x}})\boldsymbol{\delta} \|^2} \tag{47}$$

where $\boldsymbol{\delta} = \mathbf{x} - \hat{\mathbf{x}}$. Related to these relative curvature measures are the scale-free [2] and the direct curvature measures [9]. The scale-free PEC and IC are obtained by multiplying the relative measures by the standard radius ρ defined as

$$\rho = \| \mathbf{z} - f(\hat{\mathbf{x}}) \| \sqrt{\frac{N}{M-N}} \tag{48}$$

That is the scale-free PEC and IC are defined respectively as [2]

$$\gamma_\delta^{\mathrm{T}} = \rho K_\delta^{\mathrm{T}} \tag{49}$$

$$\gamma_\delta^{\mathrm{N}} = \rho K_\delta^{\mathrm{N}} \tag{50}$$

The direct PEC and IC are defined as [9]

$$\beta_\delta^{\mathrm{T}} = \frac{\| \boldsymbol{\delta}^T \ddot{F}^{\mathrm{T}}(\hat{\mathbf{x}})\boldsymbol{\delta} \|}{\| \dot{F}^{\mathrm{T}}(\hat{\mathbf{x}})\boldsymbol{\delta} \|} \tag{51}$$

$$\beta_\delta^{\mathrm{N}} = \frac{\| \boldsymbol{\delta}^T \ddot{F}^{\mathrm{N}}(\hat{\mathbf{x}})\boldsymbol{\delta} \|}{\| \dot{F}^{\mathrm{T}}(\hat{\mathbf{x}})\boldsymbol{\delta} \|} \tag{52}$$

Using the above definitions it is straightforward to evaluate these curvature measures for TOA and TDOA processing described in Section 2.

One can observe that all of the curvature measures described in this section compare the magnitude of the quadratic term to that of the linear term. The linear approximation in (37) is accurate only if the magnitude of the quadratic term is small compared to that of the linear term, i.e., the model functions with smaller curvature measures better approximate the true function value.

5 Experimental Results

The local positioning platform that we have developed at CSIRO, called WASP (Wireless Ad hoc System for Positioning), operates in the 5.8 GHz frequency band and provides both ranging and communications capabilities. It uses low-cost hardware and sophisticated signal processing to overcome the challenges due to such hardware, and provides accurate ranging performance in both indoor and outdoor environments. Details of this platform can be found in [5].

We collected data using the WASP platform to evaluate the performance of both the TOA and TDOA processing techniques. In this trial we deployed a network of WASP nodes in an outdoor environment and determined the true location of each node using conventional survey techniques. For processing twelve of these nodes were treated as anchors and the remaining nodes as mobile nodes, whose locations were to be estimated using the TOA and TDOA processing techniques.

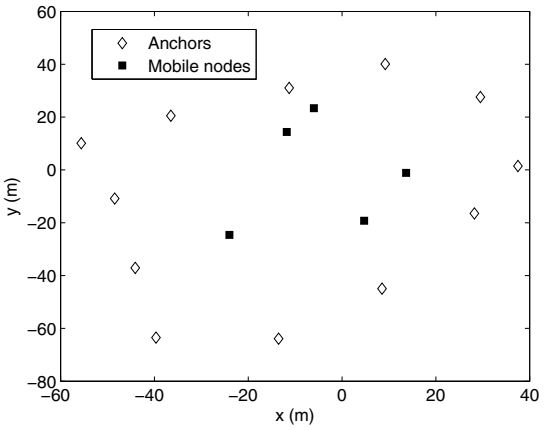

Figure 1: Locations of the anchor nodes and the mobile nodes used in the trial.

Fig. 1 shows the anchor node locations and 5 of the 25 mobile locations at which data was collected. For each mobile node several sets of data were collected, where a data set corresponds to all the measured pseudo-ranges to the anchors. Note that, unlike simulation studies, not all data sets will have the pseudo-range measurement between a mobile node and all the anchors, due to radio propagation effects. Therefore the number of anchors used to localize a mobile node may not be equal in all data sets.

Locations of the mobile nodes were estimated using both TOA and TDOA processing with ILS algorithm used for the maximization of the likelihood functions. The root mean square error (RMSE) at each of the 25 locations were calculated and it was found that the median RMSE was 0.15 m when using TOA processing and 0.24 m when using TDOA. Although for many mobile node locations the performance of both these formulations were similar, in some locations, including the five shown in Fig.1, the localization accuracy of TOA processing was significantly better compared to that of TDOA processing. In none of these locations did the TDOA processing give significantly better accuracy. Fig. 2, shows the RMSE of the location estimates at the five locations shown in Fig. 1 and the CRLB of the location estimates. As the true location of all nodes is known the actual range noise variance can be determined and was used for the CRLB estimate.

Since we have already shown that the CRLB of the two formulations are the same and that both used the same pseudo-range measurements and the same algorithm for optimization of the ML cost function, one would expect to get the same localization accuracy from the two formulations. As seen from Fig. 2, however, there is a significant difference in the estimation accuracy.

At each iteration, since the ILS algorithm approximates the cost function by a first-order Taylor series and solves a linear least squares problem, one can expect that the greater

the nonlinearity of the cost function the greater the difficulty in finding the global minima. Since the curvature measures described in Section 4 quantify the nonlinearity and hence the accuracy of the first-order approximation, we calculated these measures for both the TOA and TDOA formulations.

The relative, scale-free, and direct PEC and IC measures were calculated for all the data sets of different mobile nodes, and the median values of relative and scale-free curvatures of the third mobile node are shown Fig. 3 and the corresponding direct curvature measures in Fig. 4. For all nonlinearity measures the TDOA processing presents a significantly greater value compared that of TOA. This leads to increased localization error for TDOA processing.

We observed in all the 25 locations that the curvature measures of the TOA processing were lower than that of the TDOA processing. Further, increasing the number of iterations in the ILS algorithm did not change the localization accuracy. Therefore, we conclude that the increased nonlinearity of the TDOA processing causes the ILS algorithm to get stuck in a local minimum in cases where the localization error is higher.

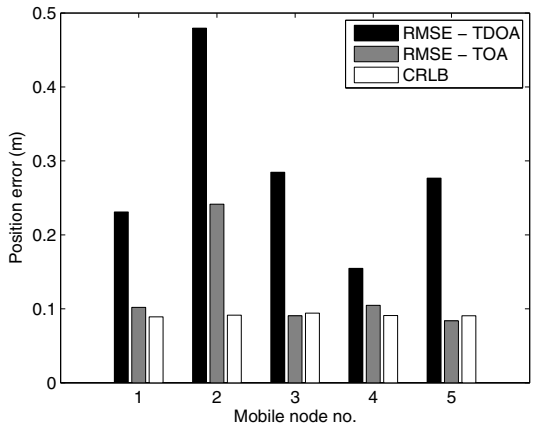

Figure 2: Comparison of RMSE for the two formulations against CRLB for the scenario shown in Fig. 1.

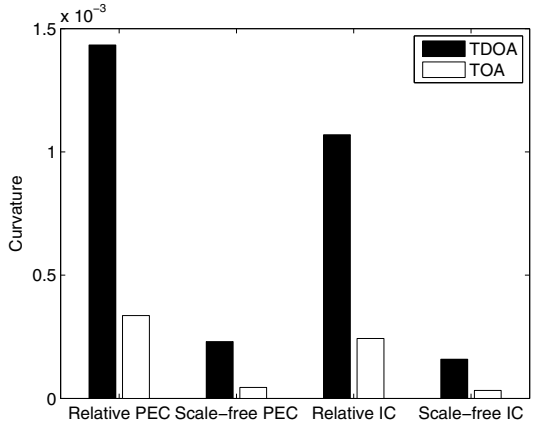

Figure 3: Relative and scale-free curvature measures for the third mobile node.

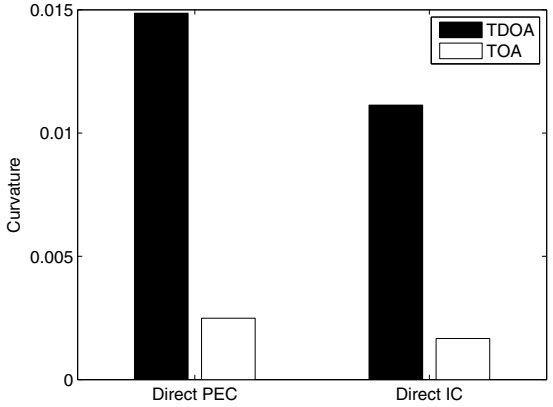

Figure 4: Direct curvature measures for the third mobile node.

6 Conclusions

The error characteristics of the TOA and TDOA processing methods for localization using pseudo-range measurements was analyzed in this paper. We analytically proved that the CRLB of these two formulations is the same and hence one would expect to obtain the same localization accuracy by considering either of the two formulations. In our experimental study, however, the TDOA processing, which is the widely used in local positioning systems [3],[6],[14], resulted in reduced localization accuracy compared to the TOA processing. By analyzing the nonlinearity of the two formulations using the differential geometry-based curvature measures, we showed that the nonlinearity of the TDOA processing is higher compared to that of the TOA processing, which leads to the degradation in the localization accuracy. Hence, our analysis shows that, contrary to the popularity of TDOA processing, TOA processing is the better formulation for pseudo-range localization.

Acknowledgement

We would like to thank Alija Kajan for organizing the data collection.

Appendix

A Calculation of the FIM in TDOA Processing

By double differentiating the Gaussian measurement likelihood given in (7) and taking the expectation we can show that

$$\mathbb{E}\left\{\frac{\partial^2 \log p(\mathbf{r}_d|\mathbf{p})}{\partial x^2}\right\} = -\frac{\partial \boldsymbol{\alpha}}{\partial x}^T R_{TD}^{-1} \frac{\partial \boldsymbol{\alpha}}{\partial x} \qquad (53)$$

$$\mathbb{E}\left\{\frac{\partial^2 \log p(\mathbf{r}_d|\mathbf{p})}{\partial y^2}\right\} = -\frac{\partial \boldsymbol{\alpha}}{\partial y}^T R_{TD}^{-1} \frac{\partial \boldsymbol{\alpha}}{\partial y} \tag{54}$$

$$\mathbb{E}\left\{\frac{\partial^2 \log p(\mathbf{r}_d|\mathbf{p})}{\partial x \partial y}\right\} = -\frac{\partial \boldsymbol{\alpha}}{\partial x}^T R_{TD}^{-1} \frac{\partial \boldsymbol{\alpha}}{\partial y} \tag{55}$$

where $\boldsymbol{\alpha} = \mathbf{r}_d - \boldsymbol{\mu}_{TD}$.

The partial derivatives of α_i with respect to x and y is easily evaluated to

$$\frac{\partial \alpha_i}{\partial x} = -\frac{(x - x_{i'})}{\|\mathbf{p} - \mathbf{p}_{i'}\|} + \frac{(x - x_1)}{\|\mathbf{p} - \mathbf{p}_1\|} \tag{56}$$

$$\frac{\partial \alpha_i}{\partial y} = -\frac{(y - y_{i'})}{\|\mathbf{p} - \mathbf{p}_{i'}\|} + \frac{(y - y_1)}{\|\mathbf{p} - \mathbf{p}_1\|} \tag{57}$$

where $i = 1, 2, \cdots, N-1$ and $i' = i + 1$.

To analytically evaluate the elements of the FIM the inverse of the covariance matrix R_{TD} given in (6) is required, which can be evaluated using the following lemma [10].

Lemma 1. *If G and H are two matrices such that G is invertible and H has rank 1, then*

$$(G + H)^{-1} = G^{-1} - \frac{1}{1 + g} G^{-1} H G^{-1} \tag{58}$$

where $g = tr\, H G^{-1}$.

We can write R_{TD} as

$$R_{TD} = \begin{bmatrix} \sigma_2^2 & 0 & \dots & 0 \\ 0 & \sigma_3^2 & \dots & 0 \\ \vdots & \vdots & \vdots & \vdots \\ 0 & 0 & \dots & \sigma_N^2 \end{bmatrix} + \begin{bmatrix} \sigma_1^2 & \sigma_1^2 & \dots & \sigma_1^2 \\ \sigma_1^2 & \sigma_1^2 & \dots & \sigma_1^2 \\ \vdots & \vdots & \vdots & \vdots \\ \sigma_1^2 & \sigma_1^2 & \dots & \sigma_1^2 \end{bmatrix} \tag{59}$$

$$= R_1 - R_2 \tag{60}$$

R_1 is a diagonal matrix and has inverse and R_2 is a matrix that has rank 1. Then Lemma 1 can be used to find R_{TD}^{-1}, which is given by

$$R_{TD}^{-1} = \begin{bmatrix} 1/\sigma_2^2 & 0 & \dots & 0 \\ 0 & 1/\sigma_3^2 & \dots & 0 \\ \vdots & \vdots & \vdots & \vdots \\ 0 & 0 & \dots & 1/\sigma_N^2 \end{bmatrix} - \frac{\sigma_1^2}{1 + g} \begin{bmatrix} 1/\sigma_2^4 & 1/\sigma_2^2\sigma_3^2 & \dots & 1/\sigma_2^2\sigma_N^2 \\ 1/\sigma_3^2\sigma_2^2 & 1/\sigma_3^4 & \dots & 1/\sigma_3^2\sigma_N^2 \\ \vdots & \vdots & \vdots & \vdots \\ 1/\sigma_N^2\sigma_2^2 & 1/\sigma_N^2\sigma_3^2 & \dots & 1/\sigma_N^4 \end{bmatrix} \tag{61}$$

where $g = \sigma_1^2 \sum_{i=2}^{N} 1/\sigma_i^2$.

Now substituting the above for R_{TD}^{-1} in (53), (54), and (55) and after some straightforward, but tedious, calculations we can derive the elements of the FIM as given in (23), (24), and (26).

References

[1] Y. Bar-Shalom, X. R. Li, and T. Kirubarajan, *Estimation with Applications to Tracking and Navigation*. New York, NY: John Wiley & Sons, 2001.

[2] D. M. Bates and D. G. Watts, "Relative curvature measures of nonlinearity," *Journal of the Royal Statistical Society. Series B (Methodological)*, vol. 42, no. 1, pp. 1–25, 1980.

[3] Y. Chan and K. Ho, "A simple and efficient estimator for hyperbolic location," *IEEE Trans. Signal Process.*, vol. 42, no. 8, pp. 1905–1915, Aug. 1994.

[4] W. H. Foy, "Position-location solutions by Taylor-series estimation," *IEEE Trans. Aerosp. Electron. Syst.*, vol. AES-12, p. 187194, Mar. 1976.

[5] M. Hedley, D. Humphrey, and P. Ho, "System and apparatus for accurate indoor tracking using low-cost hardware," in *Proc. Position Location And Navigation Symposium*, Monterey, CA, May 2008, pp. 633–640.

[6] Y. Huang, J. Benesty, G. W. Elko, and R. M. Mersereau, "Real-time passive source localization: a practical linear-correction least-squares approach," *IEEE Trans. Speech Audio Processing*, vol. 9, pp. 943–956, Nov. 2001.

[7] E. D. Kaplan, *Understanding GPS: Principles and Applications*. Boston, MA: Artech House, 1996.

[8] S. M. Kay, *Fundamentals of Statistical Signal Processing: Estimation Theory*. Upper Saddle River, NY: Prentice Hall, 1993.

[9] B. La Scala, M. Mallick, and S. Arulampalam, "Differential geometry measures of nonlinearity for filtering with nonlinear dynamic and linear measurement models," in *Proc. SPIE Signal and Data Processing of Small Targets*, San Diego, CA, 2007, pp. 66 990C–1–66 990C–12.

[10] K. S. Miller, "On the inverse of the sum of matrices," *Mathematics Magazine*, vol. 54, no. 2, pp. 67–72, Mar.

[11] K. Pahlavan, X. Li, and J.-P. Makela, "Indoor geolocation science and technology," *IEEE Commun. Mag.*, vol. 40, no. 2, pp. 112–118, Feb. 2002.

[12] G. A. F. Seber and C. J. Wild, *Nonlinear Regression*. Hoboken, NJ: John Wiley & Sons, 2003.

[13] D.-H. Shin and T.-K. Sung, "Comparisons of error characteristics between TOA and TDOA positioning," *IEEE Trans. Aerosp. Electron. Syst.*, vol. 38, no. 1, pp. 307–311, Jan. 2002.

[14] J. O. Smith and J. S. Abel, "Closed form least squares source location estimation from range difference measurements," *IEEE Trans. Acoustics, Speech and Signal Processing*, vol. 35, pp. 1661–1669, Dec. 1987.